Eur. Phys. J. D **34**, 169–172 (2005)
DOI: 10.1140/epjd/e2005-00139-0

THE EUROPEAN PHYSICAL JOURNAL D

Negative ion photoelectron spectroscopy of 2,2'-bithiophene cluster anions, $(2T)_n^-$ (n = 1–100)

M. Mitsui[1], Y. Matsumoto[1], N. Ando[1], and A. Nakajima[1,2,a]

[1] Department of Chemistry, Faculty of Science and Technology, Keio University, 3-14-1 Hiyoshi, Kohoku-ku, Yokohama 223-8522, Japan
[2] CREST, Japan Science and Technology Agency, c/o Department of Chemistry, Keio University, Yokohama 223-8522, Japan

Received 6 September 2004
Published online 13 July 2005 –

Abstract. Cluster anions of 2,2'-bithiophene, $(2T)_n^-$, were produced up to $n \sim 500$ in the gas-phase. The energetics of the excess electron in the $(2T)_n^-$ clusters with $n = 1-100$ were explored by negative ion photoelectron spectroscopy. When the vertical detachment energies (VDEs) obtained from the photoelectron spectra were analyzed by a plot against $n^{-1/3}$, it has been revealed that the excess electron trapping level thus extrapolated is located at ∼0.8 eV below the conduction band minimum (i.e. LUMO) of the 2T thin film. The large slope of the VDEs vs. $n^{-1/3}$ plot suggests that the neutral 2T molecules surrounding the anion core take non-planar twisted conformations with permanent dipole moments, resulting in the exceedingly deep trapping of the excess electron in the 2T cluster anions.

PACS. 36.40.-c Atomic and molecular clusters – 36.40.Wa Charged clusters

1 Introduction

Oligothiophene compounds have received widespread attention as attractive organic materials used in a variety of applications in electronics and optoelectronics such as light emitting diodes [1], field effect transistors [2], and photovoltaic cells [3]. Understanding the structural and electronic peculiarities of oligothiophenes and their aggregates is thus one of important subjects to control their charge transport and optical properties.

The 2,2'-bithiophene (2T) is the smallest building block (apart from the thiophene monomer) and has been extensively investigated as a useful model for the properties of longer oligothiophenes. For examples, gas-phase electron diffraction experimental data show that 2T exists in two nonplanar conformation, syn-gauche and anti-gauche, with torsional angles of $36 \pm 5°$ and $148 \pm 3°$ [4]. Molecular electron affinity as well as energetic positions of singlet and triplet states of 2T has been revealed by high resolution negative ion photoelectron spectroscopy [5]. Unoccupied and occupied electronic states of thin film of 2T have been also investigated by ultraviolet photoelectron spectroscopy and inverse photoelectron spectroscopy [6].

Gaseous clusters can provide microscopic aspects of local structures and electronic properties of condensed media. In particular, wide size range studies of clusters enables us to bridge the gap between microscopic and macroscopic phenomena. Despite the numerous experimental and theoretical studies on 2T [4–10], the clusters of 2T have been never studied up to date. In this article, we present the photoelectron spectroscopic study on gaseous nanometer scale cluster anions of 2T, $(2T)_n^-$ ($n = 1-100$). The structure and electronic properties of 2T molecular anion have been revealed by photoelectron spectroscopy and theoretical calculations. Specifically, the experimental slope obtained by the vertical detachment energies (VDEs) versus $n^{-1/3}$ plot is much larger than those of the negatively charged non-dipolar clusters, e.g. $(\text{benzene})_n^-$ [11,12] and comparable to those of the dipolar clusters, e.g. $(CH_3CN)_n^-$ [13] and $(NH_3)_n^-$ [14], suggesting the non-planar twisted conformations of the neutral 2T molecules surrounding the anion core.

2 Experimental section

Details of the experimental apparatus are given in references [15]. In short, the solid sample of 2,2'-bithiophene (2T) was placed in a sample holder heated up to ∼100 °C to obtain sufficient sample vapor. The sample vapor was entrained in helium carrier gas at a stagnation pressure of 50−100 atm and was pulsed out through a Even-Lavie valve [16] into a vacuum chamber at a 10 Hz repetition rate. Anions were produced by attachment of slow secondary electrons generated by high-energy electron impact (∼500 eV) ionization at the condensation zone in a free jet.

[a] e-mail: nakajima@chem.keio.ac.jp

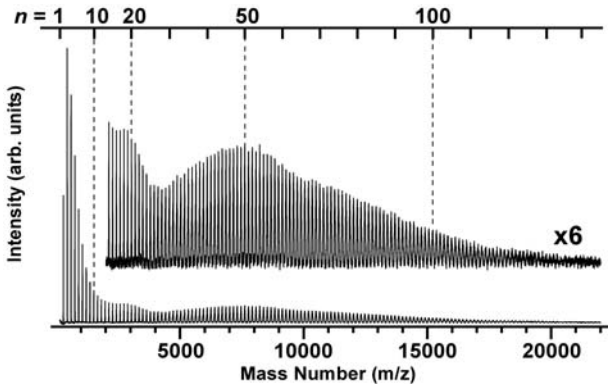

Fig. 1. Mass spectrum of 2T cluster anions.

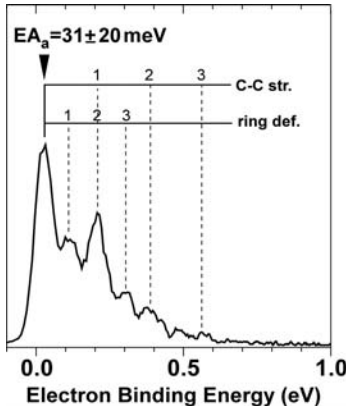

Fig. 2. Photoelectron spectrum of 2T anion ($2T^-$) taken at 1064 nm.

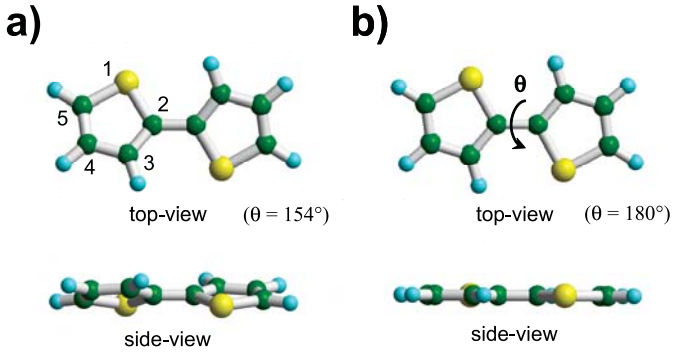

Fig. 3. The optimized structures of 2T neutral (a) and anion (b) calculated at the B3LYP/6-311++G** level.

The anions, $(2T)_n^-$, were continued through a skimmer to a linear time-of-flight mass spectrometer (TOF-MS), where a pulsed electric field directed the cluster anions toward a magnetic bottle photoelectron analyzer [15]. For 2T anion ($2T^-$) and small $(2T)_n^-$ clusters ($n = 2$–8), the anions were impulsively decelerated before being crossed with a photodetachment laser. For larger clusters ($n \geq 9$), the anions were not decelerated, because the photoelectron spectra obtained without deceleration were nearly the same with the spectra with deceleration. In this study, three detachment photon energies were used, 1064 nm (1.165 eV), 532 nm (2.331 eV), and 355 nm (3.496 eV). The photoelectron spectra represented an accumulation of 3,000−10,000 laser shots. Typical energy resolution of our photoelectron spectrometer is ∼50 meV FWHM (full width at half maximum) at 1 eV electron kinetic energy. The photoelectron energy was calibrated with the $^1S_0 \rightarrow {}^2S_{1/2}$ and $\rightarrow {}^2S_{3/2}$ transitions of the gold atomic anion.

3 Results and discussion

3.1 Mass spectrum of 2,2'-bithiophene cluster anions

Figure 1 shows mass spectrum of $(2T)_n^-$ clusters recorded with the high helium stagnation pressure of 100 atm. The cluster anions are formed up to $n \simeq 150$. In our TOF-MS measurement, however, the detectable mass is limited up to ∼25,000 u [i.e. $(2T)_n^-$ with $n \lesssim 150$] due to lower velocities of larger cluster anions and limited sensitivity of ion detector. It should be noted that the photoelectron signal can be detected up to $n \simeq 500$ in the photoelectron measurement, indicating the formation of $(2T)_n^-$ clusters up to $n \simeq 500$ under the current experimental condition. Assuming a spherical cluster shape, the diameter of $(2T)_{500}^-$ clusters is larger than 4 nm.

3.2 Photoelectron spectrum and theoretical calculation of 2,2'-bithiophene anion, $2T^-$

Figure 2 shows the photoelectron spectrum of $2T^-$ measured with detachment wavelengths of 1064 nm. The origin peak is observed at 31±20 meV, which agrees with the adiabatic electron affinity (EA_a) value of a 2T molecule determined by Weinkauf et al., $EA_a = 49 \pm 5$ meV [5]. The two prominent vibrational progressions were also observed with a spacing of 82 meV (∼660 cm^{-1}) and 175 meV (∼1410 cm^{-1}) which were tentatively assigned to ring deformation and C-C stretching modes, respectively [6].

Although many theoretical studies on neutral 2T molecule have been reported [6,8–10], there have been few calculations on the anions. Exploratory density functional theory (DFT) calculations were carried out to gain insight into the nature of $2T^-$. All calculations of the equilibrium geometries, energies and harmonic vibrational frequencies were done using a suite of Gaussian 98 programs [17]. Figure 3 shows global minimum structures at the B3LYP/6-311++G** level of theory for neutral (a) and anion (b) of 2T. In both the neutral and anion, the *anti-gauche* conformer is the most stable, though their torsional angles are different. The neutral *anti-gauche* conformer possesses nonplanar twisted conformation with torsional angle (θ) of 154° which agrees well with the experimental data of 148±3° determined by gas-phase electron diffraction measurement [4]. On the other hand, the *anti-gauche* conformer anion takes planar C_{2h} structure. The significant geometry changes in the anion compared to the neutral are found in the lengthening of the S_1–C_2 (0.039 Å), C_2–C_3 (0.036 Å) and C_4–C_5 (0.012 Å) bonds and the shortening of the C_3–C_4 (0.015 Å) and inter-ring C–C bond

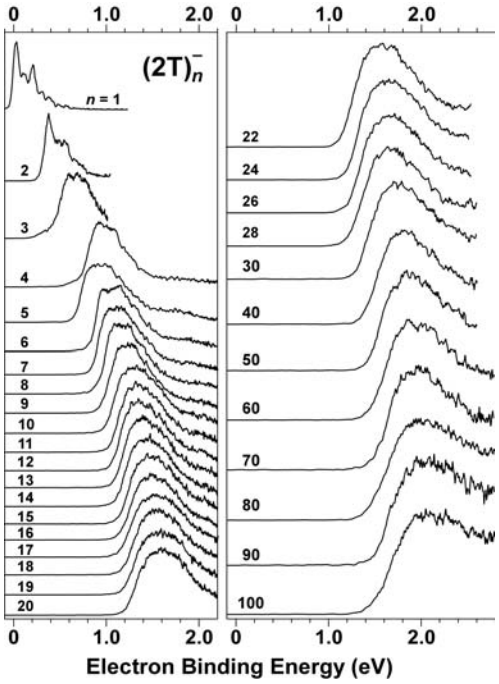

Fig. 4. Photoelectron spectra of $(2T)_n^-$ ($n = 1-100$) taken at 1064 nm for $n = 1-3$, 532 nm for $n = 4-20$, and 355 nm for $n = 22-100$.

(0.046 Å). As shown in Figure 2, the two vibrational progressions of the ring deformation and C–C stretch were clearly observed in the spectrum, which are compatible well with the calculated geometry changes from the anion to the neutral. The torsional mode should be also excited in the photodetachment process, since the torsional angle changes from the anion to the neutral. However, the energy of torsion is only ∼5 meV [6], which cannot be resolved with the limited energy resolution of our photoelectron spectrometer.

3.3 Photoelectron spectra of 2,2'-bithiophene cluster anions

Figure 4 shows the photoelectron spectra of $(2T)_n^-$ ($n = 1-100$) measured with detachment wavelengths of 1064 nm for $n = 1-3$, 532 nm for $n = 4-20$ and 355 nm for $n = 22-100$. The partially resolved vibrational features of C–C stretching modes were also observed in the spectra of $(2T)_2^-$. In the photoelectron spectra of larger clusters ($n \geq 3$), however, the vibrational features become unresolved and the bandwidth becomes broad with the cluster size, because the number of intermolecular vibrational modes excited in the photodetachment process increases with the size. Although the irregular shift is observed from $n = 4$ to 5, the vertical detachment energy (VDE) of cluster anions ($n = 6-100$) is shifted monotonically toward higher electron binding energy as the cluster size increases.

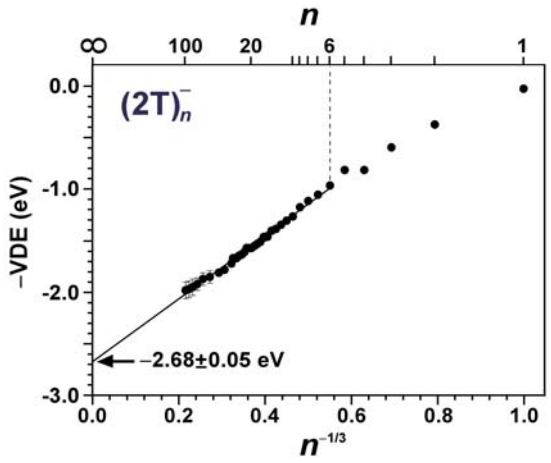

Fig. 5. Plot of VDEs of $(2T)_n^-$ ($n = 1-100$) as a function of $n^{-1/3}$. The VDEs for $n = 6-100$ are all fitted linearly with $n^{-1/3}$ and are extrapolated to intercepts [VDE(∞)] of 2.68 ± 0.05 eV.

3.4 VDE versus $n^{-1/3}$ plot: extrapolation from cluster to bulk

The cluster size n can be related to the radius of the spherical cluster (R) by $R = r_s n^{1/3}$, where r_s is the effective radius of a single constituent molecule, and thus VDE data obtained from photoelectron spectra are plotted against $n^{-1/3}$ instead of R^{-1}. Figure displays the plot of experimental VDEs as a function of $n^{-1/3}$ for $(2T)_n^-$ with $n = 1-100$. The VDEs of $n \geq 6$ are well fitted linearly against $n^{-1/3}$ and solid line in Figure 5 represents the least square fit of the VDE data: $-\text{VDE} = -2.68 + 3.05n^{-1/3}$ (correlation coefficient; 0.997).

The extrapolated value of VDE, i.e. VDE(∞), could be related to the energy of conduction band minimum (i.e. the lowest unoccupied molecular orbital (LUMO)). Since the VDE corresponds to — the energy required to remove the excess electron vertically from the anion in the ground state to infinity, the VDE — involves total reorganization energy (λ_{tot}). The λ_{tot} energy is the sum of two relaxation energies of (1) nuclear reorganizations from the equilibrium geometry of the neutral state to that of the anion state (λ_1) and (2) those from the equilibrium geometry of the anion state to that of the neutral state (λ_2); $\lambda_{\text{tot}} = \lambda_1 + \lambda_2$. Hence, VDE is given by

$$\text{VDE} \approx EA_{\text{a}} + P^- + \lambda_{\text{tot}}, \quad (1)$$

where P^- represent the effective polarization energy. The nuclear reorganization processes (1) and (2) mentioned above involve the same geometric changes along intermolecular coordinates, so that we assumed to be $\lambda_1 \approx \lambda_2$. Based on this assumption, the excess electron trapping level from the vacuum level (E_{Tr}) is given by

$$-E_{\text{Tr}} \approx EA_{\text{a}} + P^- + \lambda_{\text{tot}}/2 = \text{VDE}(\infty) - \lambda_{\text{tot}}/2. \quad (2)$$

On the other hand, the energy of the LUMO from the vacuum level in molecular solid [18] is given by

$$-E_{\text{LUMO}} \approx EA_{\text{a}} + P^- = \text{VDE}(\infty) - \lambda_{\text{tot}}. \quad (3)$$

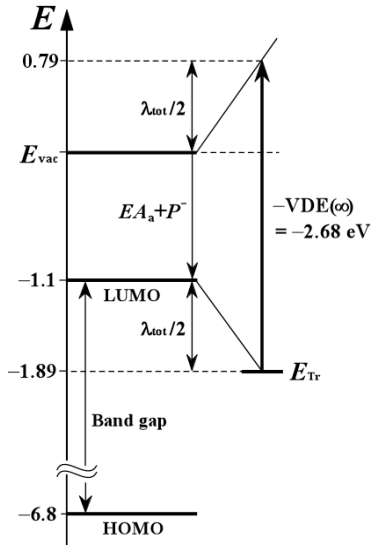

Fig. 6. A schematic energy level diagram of 2T, together with the excess electron trapping level ($E_{\rm Tr}$) obtained in this study. $E_{\rm vac}$, P^- and $\lambda_{\rm tot}$ represent the vacuum level, the effective polarization energy, and the total reorganization energy, respectively. See text for further discussion.

The $E_{\rm LUMO}$ value of 2T thin film has been reported to be $\sim$−1.1 eV, directly determined by inverse photoemission spectroscopy [6]. Using this literature value, we can approximately obtain the $\lambda_{\rm tot}/2$ and $E_{\rm Tr}$ values from equations (2) and (3), and the schematic energy level diagram is shown in Figure 6, where the energetics include the highest occupied molecular orbital (HOMO) and the LUMO of 2T system relative to the vacuum level ($E_{\rm vac}$), together with the excess electron trapping level ($E_{\rm Tr}$) residing in the band gap. It is found that there is large energy difference between $E_{\rm LUMO}$ and $E_{\rm Tr}$ values, which is about 0.8 eV. The bottom-up production of cluster anions is likely to produce cluster anions having a fully relaxed equilibrium geometry, since cluster anions grow with an anion core being sequentially stabilized through interaction between the anion and surrounding neutrals. Therefore, the large difference is attributed to the fact that the charge core in ionic cluster tends to be much stabilized than that in the corresponding solid: lattice distortion induced by the charge is relatively small due to its packing effect (or rigidity). In other words, the VDE(∞) value corresponds to the presumed lower limit of $E_{\rm Tr}$ in the solid.

In this study, the experimental slope of the VDE vs. $n^{-1/3}$ plot of $(2T)_n^-$ ($n = 6-100$) was determined to be 3.05. The value is much larger than those obtained for the negatively charged "non-dipolar" aromatic clusters, e.g. 1.38 for $(\text{benzene})_n^-$ [11] and 1.40 for $(\text{toluene})_n^-$ [12], while it is comparable to those of the "dipolar" clusters, e.g. 3.23 for $(CH_3CN)_n^-$ [13] and 2.83 for $(NH_3)_n^-$ [14]. According to the cluster size equations proposed by Jortner [19], larger static dielectric constant, i.e. higher polarity of the constituent molecule, results in larger slope of the VDE vs. $n^{-1/3}$ plot. Therefore, the present result suggests that the neutral 2T molecules around an anion core take non-planar twisted conformations having a permanent dipole moment, because the planar anti-conformation of 2T has a null dipole moment (i.e. non-dipolar). Although a 2T molecule is in a planar anti-conformation in the solid state due to intermolecular stacking interaction, the conformation of 2T molecules could be changed in the finite-sized clusters having intermolecular structural flexibility. Moreover, intramolecular flexibility could be contributed because it is known that torsional barrier of 2T molecule is relatively small ($\sim$0.1 eV) [9,10]. The dipolar-cluster-like behavior of the 2T cluster anions is indeed consistent with the above-mentioned result that the extrapolation of the VDEs yields the exceedingly deep trapping level of the excess electron in comparison with that in the thin film.

This work is supported by from the Ministry of Education, Culture, Sports, Science and Technology (MEXT), Grant-in-Aid for the 21st Century COE program "KEIO LCC" and for Young Scientists (B), 14740332, 2003.

References

1. F. Geiger, M. Stoldt, H. Schweizer, P. Bäuerle, E. Umbach, Adv. Mater. **5**, 922 (1993)
2. W.A. Schoonveld, J. Wildeman, D. Fichou, P.A. Bobbert, B.J. van Wees, T.M. Klapwijk, Nature **404**, 977 (2000)
3. N. Noma, T. Tsuzuki, Y. Shirota, Adv. Mater. **7**, 647 (1995)
4. S. Samdal, E.J. Samuelsen, H.V. Volden, Synth. Met. **59**, 259 (1993)
5. J. Schiedt, W.J. Knott, K.L. Barubu, E.W. Schlag, R. Weinkauf, J. Chem. Phys. **113**, 9470 (2000)
6. M. Schatzmayr, G. Koller, I. Kardinal, M.G. Ramsey, S. Stafström, F.P. Netzer, J. Chem. Phys. **110**, 8060 (1999)
7. G. Koller, R.I. Blyth, S.A. Sardar, F.P. Netzer, M.G. Ramsey, Appl. Phys. Lett. **76**, 927 (2000)
8. M. Rubio, E. Ortí, R.P. Amérigo, M. Merchán, J. Phys. Chem. A **105**, 9788 (2001)
9. P.M. Viruela, R. Viruela, E. Orti, Int. Quantum Chem. **70**, 303 (1998)
10. H.A. Duarte, H.F.D. Santos, W.R. Rocha, W.B.D. Almeida, J. Chem. Phys. **113**, 4206 (2000)
11. M. Mitsui, A. Nakajima, K. Kaya, U. Even, J. Chem. Phys. **115**, 5707 (2001)
12. M. Mitsui, A. Nakajima, K. Kaya, J. Chem. Phys. **117**, 9740 (2002)
13. M. Mitsui, S. Kokubo, N. Ando, A. Nakajima, K. Kaya, J. Chem. Phys. (to be published)
14. J.V. Coe, G.H. Lee, J.G. Eaton, S.T. Arnold, H.W. Sarkas, K.H. Bowen, C. Ludewigt, H. Haberland, D.R. Worsnop, J. Chem. Phys. **92**, 3980 (1990)
15. A. Nakajima, T. Taguwa, K. Hoshino, T. Sugioka, T. Naganuma, F. Ono, K. Watanabe, K. Nakao, Y. Konishi, R. Kishi, K. Kaya, Chem. Phys. Lett. **214**, 22 (1993)
16. U. Even, J. Jortner, D. Noy, N. Lavie, C. Cossart-Magos, J. Chem. Phys. **112**, 8068 (2000)
17. *Gaussian 98 (Revision A.11)*, edited by M.J. Frisch et al. (Gaussian, Inc., Pittsburgh PA, 2001)
18. E.A. Silinsh, *Organic molecular crystals: Their electronic states* (Springer, Berlin, 1980)
19. J. Jortner, Z. Phys. D **24**, 247 (1992), and references therein